*Clays and Clay Minerals*, Vol. 38, No. 1, 77–89, 1990.

# ANALYTICAL TRANSMISSION ELECTRON MICROSCOPE STUDIES OF PLAGIOCLASE, MUSCOVITE, AND K-FELDSPAR WEATHERING

JILLIAN F. BANFIELD[1] AND RICHARD A. EGGLETON

Department of Geology, Australian National University
P.O. Box 4, Canberra, A.C.T. 2601, Australia

**Abstract**—Analytical and high-resolution transmission electron microscopy of weathered plagioclase and K-feldspar provided microtextural and chemical data that suggest a sequential formation of weathering products. An alteration layer <1 μm thick on feldspar surfaces had short-range order and was termed protocrystalline. Relative to the parent feldspars the protocrystalline layer was depleted in Ca, Na, K, and Si and significantly enriched in Fe. On plagioclase, the protocrystalline material was replaced by Ca-Fe-K-smectite, another protocrystalline material, and spherical halloysite. Abundant tubular halloysite on the corroded surface apparently formed by reprecipitation of components released by plagioclase dissolution. The K-feldspar was markedly more resistant to weathering than the plagioclase.

Recrystallization of the patchily developed protocrystalline rind produced Fe-bearing, aluminous smectite, which was ultimately replaced by spherical halloysite and laths of kaolinite. Muscovite laths within plagioclase crystals were converted initially to illite by loss of K, then to randomly interstratified illite/smectite, and then to smectite that contained Mg, little K and Fe, and was more aluminous and contained less Ca than the smectite that originally replaced the plagioclase. Smectite was replaced epitactically by kaolinite. Kaolinite was the stable weathering product of the feldspars and muscovite in the profiles. It probably formed in equilibrium with a solution whose composition was no longer controlled by the microenvironment within the feldspar, but approached that of meteoric water.

**Key Words**—Analytical electron microscopy, High-resolution transmission electron microscopy, Illite, Kaolinite, K-feldspar, Muscovite, Noncrystalline intermediate, Plagioclase, Smectite, Weathering.

## INTRODUCTION

Feldspars are the most abundant constituents of igneous rocks; the products of their weathering form major components of sediments and soils. Numerous reports have described the mechanisms by which the structure is broken down and have documented the assemblages of secondary minerals that form under a range of environmental conditions. Various combinations of secondary minerals have been recognized; for example, feldspar has been described as weathering to a noncrystalline phase (Eswaran and Bin, 1978; Rimsaite, 1979; Eggleton and Buseck, 1980); K-feldspar to illite-muscovite (Eggleton and Buseck, 1980); to kaolinite and illite (Loughnan, 1969); to smectite (Wilson *et al.*, 1971); to smectite from an aluminous precursor (Proust and Velde, 1978); to a noncrystalline phase and smectite (Guilbert and Sloane, 1968); to kaolinite and smectite (Loughnan, 1969); to smectite, kaolinite, and gibbsite (Tardy *et al.*, 1973; Carroll, 1970); to kaolinite and gibbsite (Anand *et al.*, 1985); to kaolinite and several forms of halloysite (Keller, 1978; Wilke *et al.*, 1978); and to gibbsite (Lodding, 1972; Parham, 1969). A sequence of minerals from smectite to kaolinite and gibbsite can be predicted on thermodynamic grounds by examination of phase diagrams, such as those of Feth *et al.* (1964), Helgeson (1971), and Garrels (1984).

The concept that feldspar dissolves incongruently (Correns and Von Engelhardt, 1938) led to the hypothesis that a protective residual surface-layer develops on the altered feldspar and that reactions are controlled by diffusion through this layer. Although much work supports this view, the presence of a diffusion-limiting layer has never been demonstrated. Using X-ray photoelectron spectroscopy (XPS), Petrovic *et al.* (1976a) illustrated that a continuous precipitate layer does not develop on alkali feldspar. Holdren and Berner (1979) used scanning electron microscopy (SEM) and XPS to show that the clay on feldspar surfaces is Al-rich, hydrous, patchy, and highly permeable. They interpreted this observation to indicate that the metastable products of reaction were not diffusion-limiting and, thus, not capable of controlling the rate of feldspar dissolution. Holdren and Berner (1979) supported the idea first proposed by Lagache *et al.* (1961) that weathering of feldspar is a surface-controlled reaction. Helgeson *et al.* (1984) used transition state theory and irreversible thermodynamic calculations in further support of this conclusion.

The rate at which silicates hydrolyze is controlled by the kinetics of reactions at activated sites at which Al–O and Si–O bonds are disrupted (Aagaard and Helgeson, 1982). Many authors have argued that hydrogen is involved in the disruption of these bonds, replacing K, Na, or Ca in the feldspar structure (Fred-

[1] Present address: Department of Earth and Planetary Sciences, The Johns Hopkins University, Baltimore, Maryland 21218.

erickson, 1951; Garrels and Howard, 1959; Marshall, 1962; Wollast, 1967; Wollast and Chou, 1985). Aagaard and Helgeson (1982) summarized results indicating that it is $H_3O^+$ and not $H^+$ that enters the exchange position. A steady-state mechanism involving the creation and destruction of a critical activated complex at the surface has been proposed (Aagaard and Helgeson, 1982).

Access of a solution to the feldspar surface is probably controlled by defects, cleavages, twin planes, and cracks. Dissolution appears to proceed by preferential attack at energetically favored sites (Berner and Holdren, 1977; Nixon, 1979). Studies of surface textures of weathered minerals indicate that this mode of attack results in the formation of solution pits (Siefert, 1967; Parham, 1969; Lundstrom, 1970; Berner and Holdren, 1977).

Considerable uncertainty still exists as to whether secondary minerals precipitate from solution or crystallize from transient, noncrystalline aluminosilicate intermediates. Early investigators (e.g., Fieldes and Swindale, 1954) stated that with the exception of micas, all primary silicates pass through a noncrystalline stage in transition to secondary phases. This statement contrasts with views expressed more recently in the literature, which suggest that the dominant transformation mechanism involves dissolution and reprecipitation. For example, Tsuzuki and Kawabe (1983) suggested that a dissolution-reprecipitation mechanism may be responsible for the entire sequence from feldspar to kaolinite. Keller (1978) stated that the most logical mechanism for the production of kaolin-group minerals is via solution. Eswaran and Bin (1978) proposed that feldspar alters via solution to kaolinite and gibbsite, but via a noncrystalline stage to halloysite. Petrovic (1976b) suggested that the mechanism for the transformation of synthetic, noncrystalline precipitates that polymerize and reorder on aging is also dissolution-reprecipitation. In a recent study, however, Tazaki and Fyfe (1987) identified primitive clay and Fe compounds on, or adjacent to, surfaces of weathered feldspar.

Although several studies have been made of the artificial alteration of muscovite (e.g., t'Serstevens *et al.,* 1964; Rausell-Colom *et al.,* 1965; Lin and Clemency, 1981), few studies have described the natural weathering of this mineral. Churchman (1980) used X-ray powder diffraction (XRD) and chemical data to describe a range of mica-vermiculite-beidellite minerals and suggested that smectite inherited its octahedral sheet from muscovite.

The present study combines transmission, scanning, and analytical electron microscopy to describe the mineralogy, morphology, composition, and sequential formation of weathering products of feldspars and muscovite. The results show the presence of a previously undescribed phase lacking long-range order, which appears to be an intermediary between the feldspar and clay minerals.

## EXPERIMENTAL

### *Samples*

This study is based on weathering of K-feldspar, plagioclase, and included muscovite lamellae in the Bemboka Granodiorite and the Bullenbalong Granodiorite, southeastern New South Wales, Australia. The mineralogy, chemistry, and origin of these granodiorites were described by Beams (1980) and White *et al.* (1977). The geochemistry and mineralogy of the weathering profiles were described by Banfield (1985); the weathering of the biotite was reported by Banfield and Eggleton (1988) and of apatite by Banfield and Eggleton (1989). The weathering profile in the Bemboka Granodiorite was illustrated in Banfield and Eggleton (1989). The terms slightly, moderately, and highly weathered are used in the present paper to refer to the extent to which samples have been weathered. Intensity of weathering was estimated from the sample density and clay content, as determined by particle size analysis. Further discussion of these terms was given in Banfield and Eggleton (1989).

### *Electron microscopy*

For scanning electron microscopy, crystals of feldspar were extracted from crushed granite and saprolite, mounted on stubs, coated with either carbon or gold, and examined in a Cambridge Stereoscan 180 scanning electron microscope operated at 30 kV. An energy-dispersive X-ray spectroscopic system (EDX) provided qualitative elemental analyses, useful for distinguishing plagioclase from K-feldspar.

Samples were prepared for transmission electron microscopy (TEM) by ion-beam thinning. Ar atoms were fired at 22° to the sample from two opposing guns after ions had been accelerated across a high voltage (4–5 kV) in a vacuum of $10^{-4}$ torr. Grain-mount samples of plagioclase, K-feldspar, and their alteration products were prepared by crushing minerals and depositing a suspension of the material onto 3-mm holey carbon grids. Comparison of results from samples prepared by the two methods allowed the separation of artifacts resulting from ion-milling, such as the readily identifiable noncrystalline thin edge, from real characteristics of the specimens. Heating of the sample during ion-milling generally resulted in the collapse of smectite basal spacings to close to 10 Å, from about 12 Å as determined by XRD. Beam heating in the TEM resulted in the rapid destruction of smectite, extremely rapid destruction of kaolinite, and deformation and destruction of halloysite. Most images were obtained at comparatively low magnifications (~100,000×) and as rapidly as possible to reduce beam damage.

Electron images and diffraction patterns were obtained using a JEOL 100CX transmission electron microscope. The compositions of alteration products and parent minerals were examined using a JEOL 100CX scanning-transmission electron microscope (STEM) equipped with an energy-dispersive detector. The STEM allowed qualitative chemical analysis to be made of small areas of material (<1000 Å in diameter). Compositional data were converted to ratios of (background-subtracted) counts under major peaks. Quantitative mineral compositions obtained using an energy-dispersive Technisch Physische Dienst electron microprobe allowed the estimation of K-factors used to semiquantify analytical electron microscope (AEM) analyses. AEM data were only collected from areas that could be clearly imaged in the STEM, restricting analysis to the very thin edges of samples, thus satisfying the thin-film criteria of Cliff and Lorimer (1975).

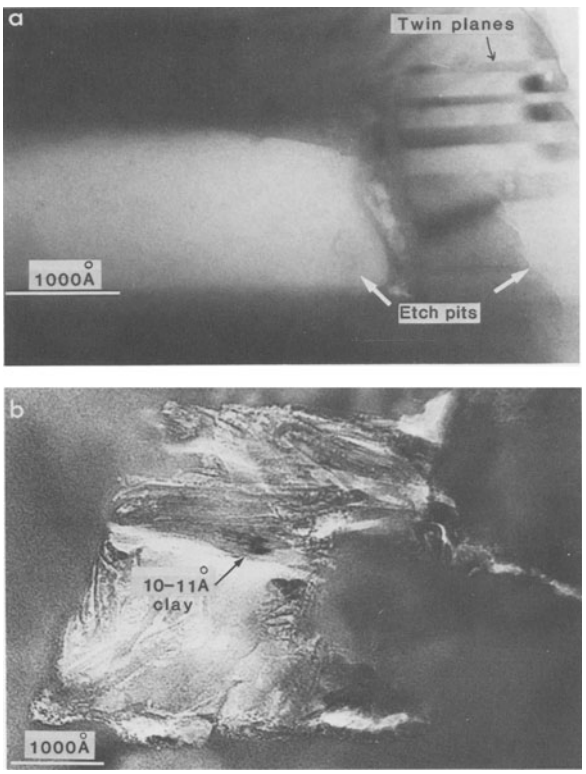


Figure 1. Transmission electron micrographs of etch pits in plagioclase: (a) pit bound by (010) twin planes, formed by dissolution of plagioclase; (b) pit containing cell-textured material and phyllosilicate, generally having basal spacings of ~11 Å, but some as large as 15 Å.

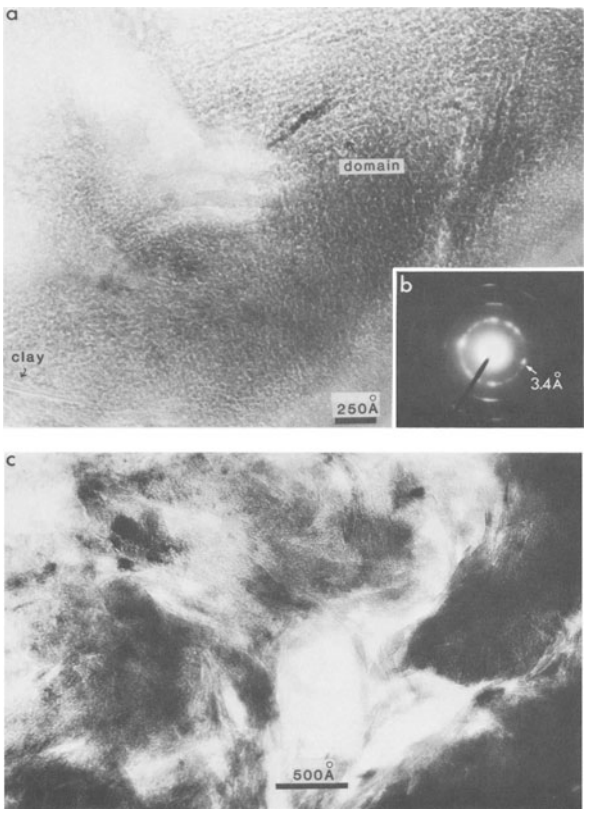


Figure 2. (a), (c) Transmission electron micrographs of cell-textured material adhering to plagioclase from the Bemboka profile showing incipient stages of recrystallization to clay; (b) selected-area electron diffraction pattern from cell-textured material with rings at 3.4, 2.3, 1.6, 1.4, 1.2 Å.

*X-ray powder diffraction*

The feldspar samples and their hydrothermal alteration and weathering products were examined by XRD using a Philips goniometer and 1010 generator operating at 40 kV and 20 mA, Co radiation, and a graphite monochromator. Halloysite was distinguished from kaolinite in samples by formamide treatment and thermal dehydration (Churchman *et al.*, 1984).

## RESULTS

### *Weathering of plagioclase*

The first stages of plagioclase weathering were identified by examination of crystals from very slightly weathered granodiorite. Electron micrographs showed etch pits located at dislocations, and on twin planes (Figure 1a) and cleavages in otherwise unaltered plagioclase. The etch pits commonly had a prismatic form, resembling negative crystals. In some pits, material resembling aggregates of tiny, equidimensional particles, here termed "cell-textured" material, coexisted with clays characterized by 10–11-Å basal spacings (Figure 1b).

In samples from more extensively weathered granodiorite, etch pits were much larger, and their margins were more irregular. A small quantity of patchily distributed cell-textured material was present adjacent to feldspar surfaces (Figures 2 and 3). The individual units in this material were 30 to 60 Å in diameter (Figure 2). The individual "cells" were partially aligned outward from the surface of the feldspar, and formed strips about 50 Å wide in poorly defined 1000-Å-wide, 2000-Å-long domains. In some areas narrow bands of clay, two or three unit cells wide, were noted in these parallel strips. The material had a cell-like texture regardless of the orientation in which it was viewed. The selected-area electron diffraction pattern (SAD) from this material (Figure 2b) contained diffuse rings and arcs at 3.4, 2.3, 1.6, 1.4, and 1.2 Å. Outward from the feldspar surface, the abundance of cell-textured material was less, and larger, curving bunches of clay having basal spacings of 10–13 Å were common (Figure 3).

In some regions the clay having the 10–13-Å basal spacing was rimmed by another cell-textured material (Figure 4). STEM analyses indicated that this cell-textured material contained considerable Fe. The cell-textured material separated smectite from aggregates of spherical clay particles, commonly about 1000 Å in diameter (Figure 4b). The spherical clay particles were abundant, commonly dominating the assemblage of

https://doi.org/10.1346/CCMN.1990.0380111 Published online by Cambridge University Press

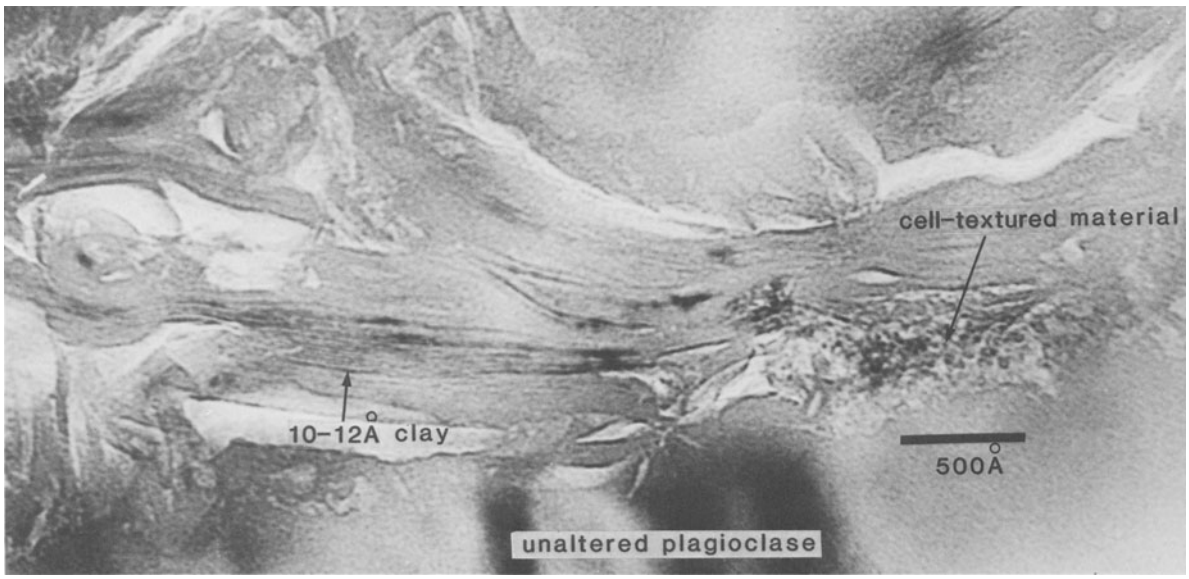


Figure 3. Transmission electron micrograph of cell-textured material developed adjacent to plagioclase from the Bemboka profile. Note the presence of phyllosilicate with 10–12-Å spacings.

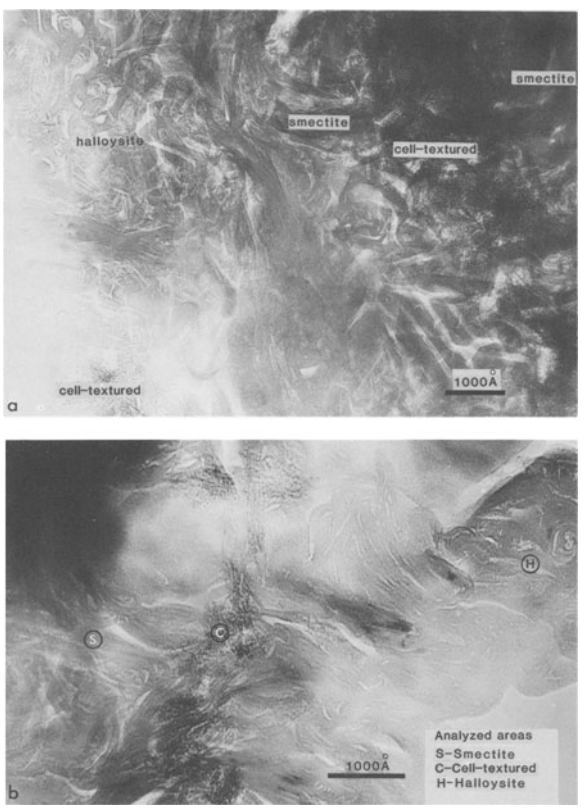


Figure 4. Transmission electron micrographs of (a) smectite, cell-textured material, and spherical halloysite occurring outward from the feldspar surface; (b) regions from which some compositions plotted in Figures 4 and 5 were obtained.

plagioclase weathering products. AEM analyses, XRD from hand-picked weathered plagioclase crystals, and SEM images of this mineral indicated that it was spherical halloysite.

Unquantified AEM data from the clay having a 10–11-Å (from SAD and measured from images) basal spacing that was interfingered with the cell-textured material are plotted on Al:Si:(K + Na + Ca) and Al:Si:Fe triangular diagrams in Figure 5. These data, in conjunction with the approximately 10-Å basal spacing (~12 Å by XRD), suggest that this alteration product was collapsed smectite.

AEM analyses illustrated that the alteration products contained abundant Ca, as well as Na and K, and that they were greatly enriched in Fe relative to the parent feldspar. Although the Ca content was not quantified (due to the lack of a suitable internal standard), it was greater than that normally encountered in smectite. No evidence for a second Ca-rich mineral was obtained. The clays ranged in composition between smectite and kaolinite. A structural formula estimated for the smectite illustrated in Figure 4b (assuming all the analyzed clay was smectite, all Fe was ferric, and calculated assuming most Ca was not in the smectite structure, e.g., assuming x was small) is:

$$(K_{0.3}Ca_x)(Fe_{0.25}Al_{3.78})\ (Si_{7.6}Al_{0.4})O_{20}(OH)_4 \cdot nH_2O.$$

Another abundant weathering product of plagioclase was noted in cavities, growing outward from the corroded plagioclase surface (Figure 6a). Its composition (Al = Si), and morphology as seen in TEM (Figure 6a) and SEM (Figures 6b and 6c) images indicated that it was almost certainly tubular halloysite. The interface between the feldspar and halloysite tubes was narrow,

https://doi.org/10.1346/CCMN.1990.0380111 Published online by Cambridge University Press

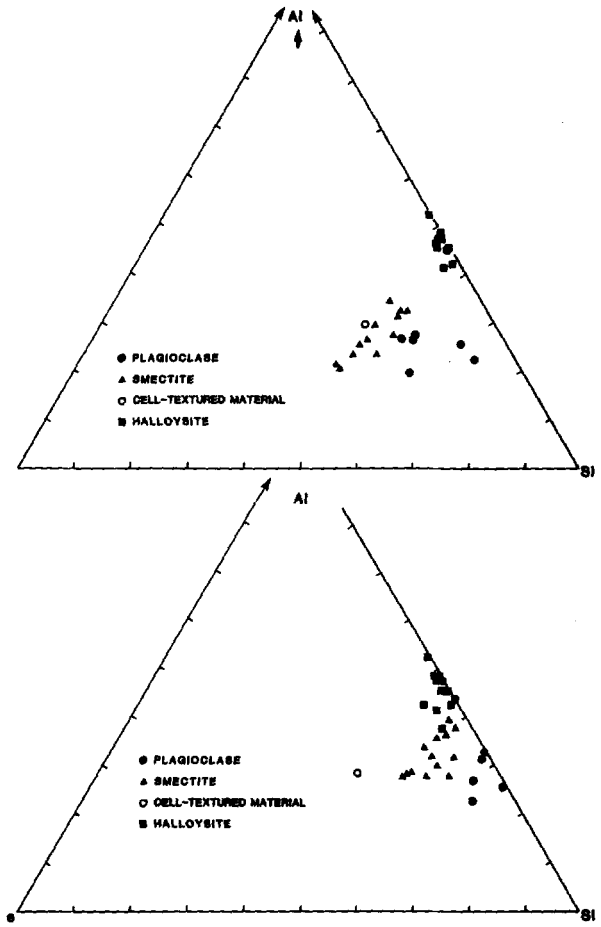


Figure 5. (upper) Triangular Al-(Ca + Na + K)-Si composition diagram for plagioclase, smectite, and cell-textured material produced by breakdown of smectite, and halloysite. Data plotted as background-subtracted counts. (lower) Triangular Al-Fe-Si composition diagram for plagioclase and weathering products considered in upper diagram.

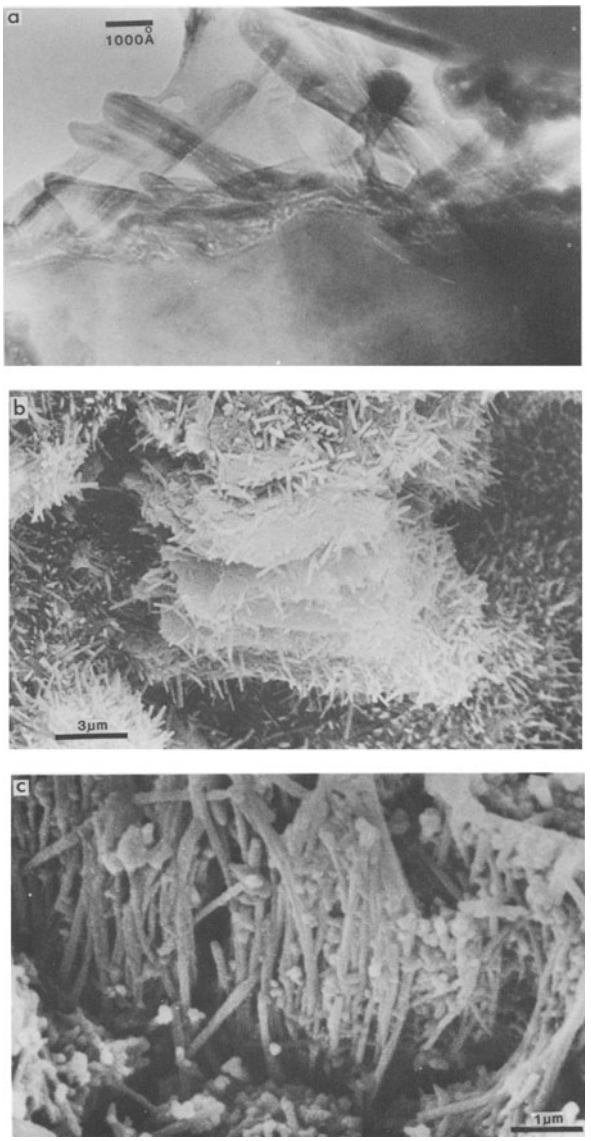


Figure 6. (a) Transmission electron micrograph of halloysite tubes adjacent to corroded feldspar surface; (b), (c) scanning electron micrographs of halloysite tubes growing outward from a solution cavity in plagioclase.

no more than 250 Å wide. Crystals of goethite, generally a few hundred Ångstroms wide, coexisted with halloysite in some areas (not illustrated).

*Weathering of muscovite*

The weathering of muscovite resulted in changes in the chemistry, basal spacings, and morphology of the lamellae. The apparent degree of weathering could also be correlated with increasing sensitivity of the phyllosilicates to damage in the electron beam. Chemical data indicated that muscovite lamellae altered initially by losing K (see Figure 10). This reaction appears to have proceeded simultaneously with, or following, alteration of the surrounding plagioclase (Figure 7). TEM images indicated that the K-deficient muscovite crystals characteristically had a more irregular shape (Figure 8) than the prismatic laths of fresh muscovite.

Electron micrographs indicated that K-depletion of muscovite was followed by the development of apparently wider (11–12 Å) layers, which were distributed randomly amongst the 10-Å-wide K-deficient muscovite layers (Figure 9). Guthrie and Veblen (1989) demonstrated that compositional differences between illite and smectite layers can produce apparent changes in basal spacings, which do not reflect structural differences. The proportion and distribution of these apparently wider layers in the altered muscovite lamellae was variable. Higher proportions of wider layers apparently correlated with more extensive weathering.

AEM analyses revealed that muscovite contained no detectable Mg and Fe. Weathering products had an Al:

https://doi.org/10.1346/CCMN.1990.0380111 Published online by Cambridge University Press

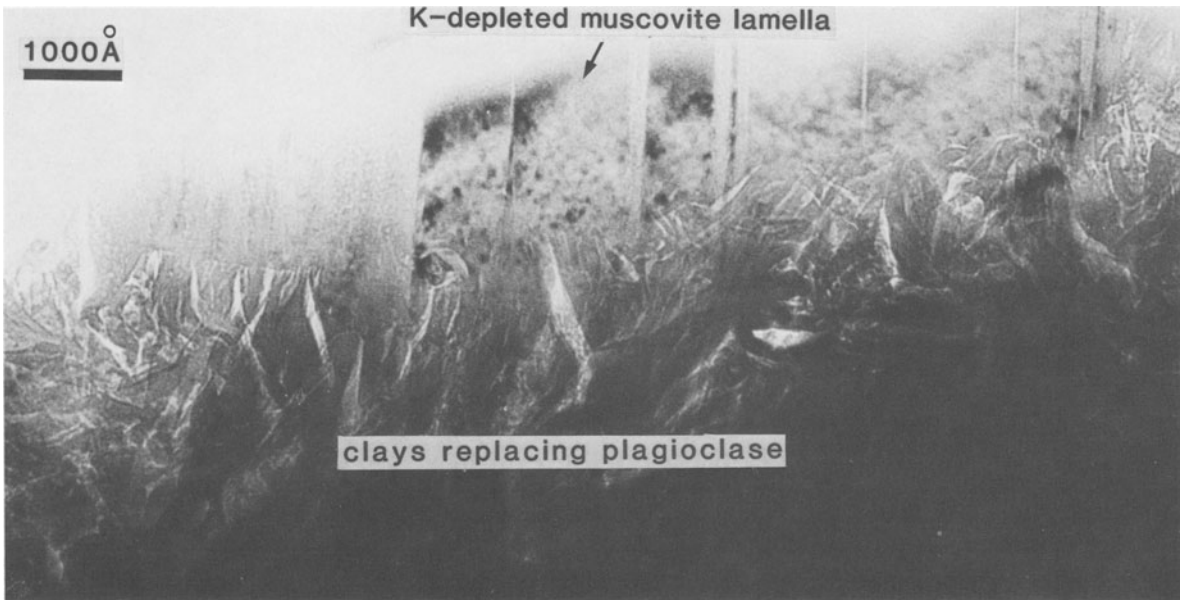


Figure 7. Transmission electron micrographs of K-deficient muscovite lamella surrounded by abundant weathering products of plagioclase.

Si ratio similar to that of muscovite; they contained considerably less K and small quantities of Mg and Fe. The basal spacings and composition of the muscovite weathering products were consistent with their being composed of randomly interstratified illite/smectite. (I/S). Compositional data for the muscovite and I/S are presented in Figure 10. The data form a trend from muscovite, toward a smectite composition that plots close to the Al-Si edge of the triangular diagram. This smectite is distinguished from that formed by the weathering of plagioclase by its higher Al:Si ratio, lower content of Ca, K, Na, and Fe, and the presence of Mg.

In more highly weathered muscovite, irregular smectite lamellae contained packets of platy kaolinite, identified in TEM images and electron diffraction patterns by 7-Å basal spacings (Figure 11). The highly weathered granodiorite contained kaolinite pseudomorphs after muscovite (AEM data in Figure 10).

*K-feldspar weathering*

Electron microscopy indicated that fresh K-feldspar (Bemboka profile) contained abundant etch pits, typically associated spatially with dislocations and twin planes. In the early stages, weathering apparently proceeded by crystallographically controlled dissolution. Etch pits were locally present on linear dislocations. Small quantities of cell-textured material similar to that found in plagioclase were present in some of these pits, commonly coexisting with phyllosilicates. It was not until most of the other minerals in the granodiorite had been extensively weathered that K-feldspar was replaced by appreciable quantities of clay.

In more highly weathered K-feldspar, strips of cell-

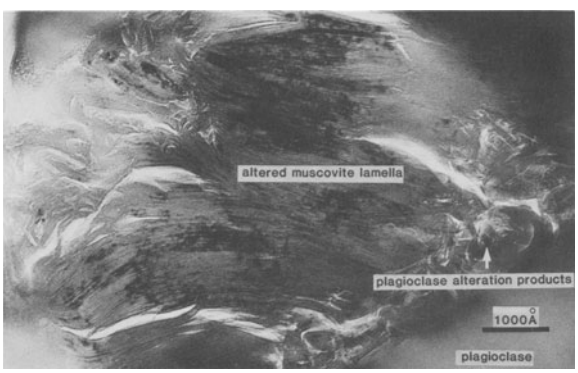


Figure 8. Transmission electron micrograph of a muscovite-illite-smectite lamella that has a more irregular morphology than that of the prismatic muscovite lamellae.

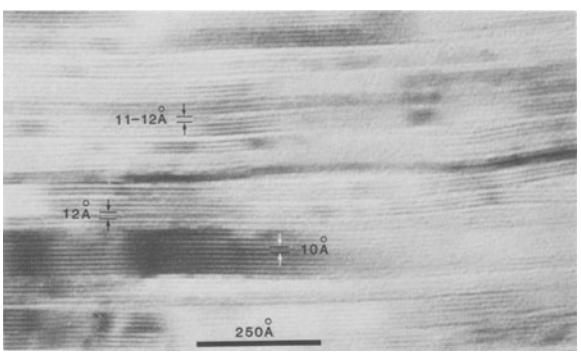


Figure 9. Transmission electron micrograph of a lamella containing sheets with basal spacings larger than those of the host muscovite-illite.

https://doi.org/10.1346/CCMN.1990.0380111 Published online by Cambridge University Press

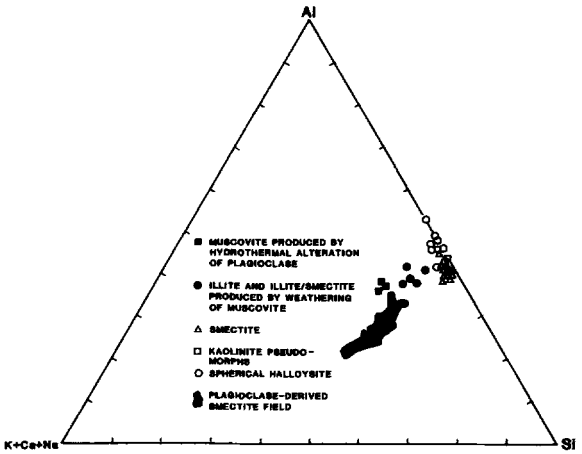


Figure 10. Triangular Al-(K + Na + Ca)-Si composition diagram comparing muscovite and its weathering products with smectite produced by weathering of plagioclase. Kaolinite data are from kaolinite pseudomorphs after muscovite.

textured material, as wide as 0.5 $\mu$m, were observed on feldspar surfaces (Figure 12). Higher magnification images from this region (Figure 13) illustrated that outward from this interface the cell-textured material was internally foliated, and individual strips of clay were present in some areas. The larger crystals of clay were identified as smectite by their composition, basal spacing in electron images, and by XRD of weathered K-feldspar crystals. The curved bands of smectite are illustrated in Figures 12, 13c, and 13d. A narrow strip of cell-textured material can be seen at most feldspar surfaces, probably a metastable intermediary between feldspar and smectite. Figures 12 and 13 illustrate the spatial relationship between K-feldspar and its weathering products. The alteration front shown in Figure 12 is irregular, extending into the feldspar along cracks and cleavage planes, leaving isolated blocks of unaltered K-feldspar.

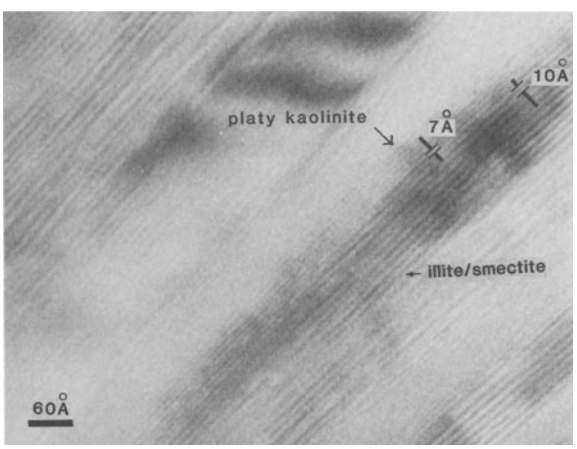


Figure 11. Transmission electron micrograph of packets of platy kaolinite intergrown with illite/smectite sheets.

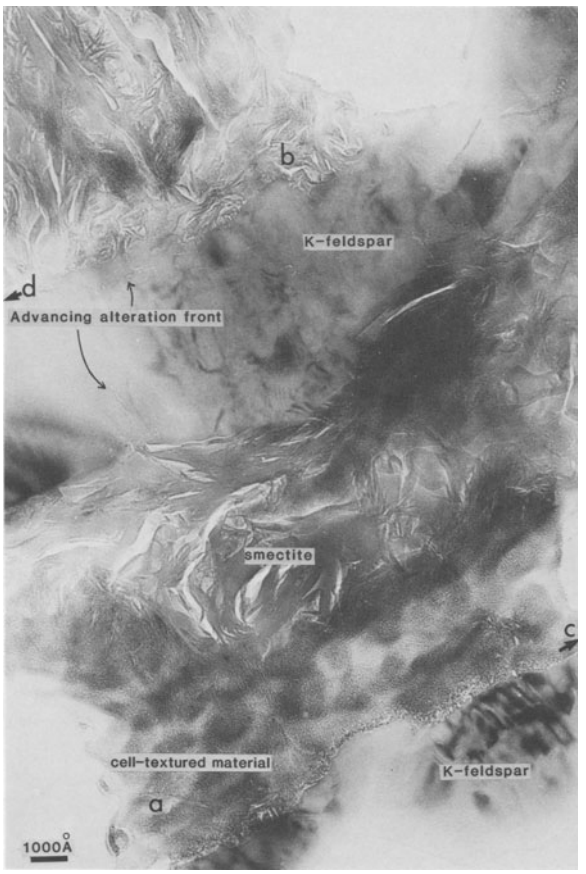


Figure 12. Transmission electron micrograph illustrating islands of K-feldspar rimmed with cell-textured material and smectite. a, b, c, d = regions enlarged in Figure 13.

Weathered K-feldspar in the Jindabyne profile was found to be characterized by many of the features described in the K-feldspar from the Bemboka profile. The Jindabyne K-feldspar also contained cell-textured material and smectite that occurred as more regular, prismatic, elongate bands than those described above.

The compositions of alteration products from the two profiles are plotted in the K:Al:Si and Fe:Al:Si triangular diagrams in Figure 14. Average compositions of the cell-textured material and smectites are given below: Bemboka cell-textured material (for point marked + in Figure 14 and expressed as smectite and Fe-hydroxide):

$$K_{0.4}(Fe_{0.9}Al_{3.1})(Si_{7.4}Al_{0.6})O_{20}(OH)_4 \cdot nH_2O(Fe_{1.3}(OH)_{3.7})$$

Bemboka smectite:

$$K_{0.4}(Mg_{small}Fe_{0.7}Al_{3.1})(Si_{7.4}Al_{0.6})O_{20}(OH)_4 \cdot nH_2O$$

Jindabyne smectite:

$$K_{0.5}(Mg_{small}Fe_{0.3}Al_{3.6})(Si_7Al_1)O_{20}(OH)_4 \cdot nH_2O.$$

The cell-textured material contained variable and, locally, very high concentrations of Fe, and the smec-

https://doi.org/10.1346/CCMN.1990.0380111 Published online by Cambridge University Press

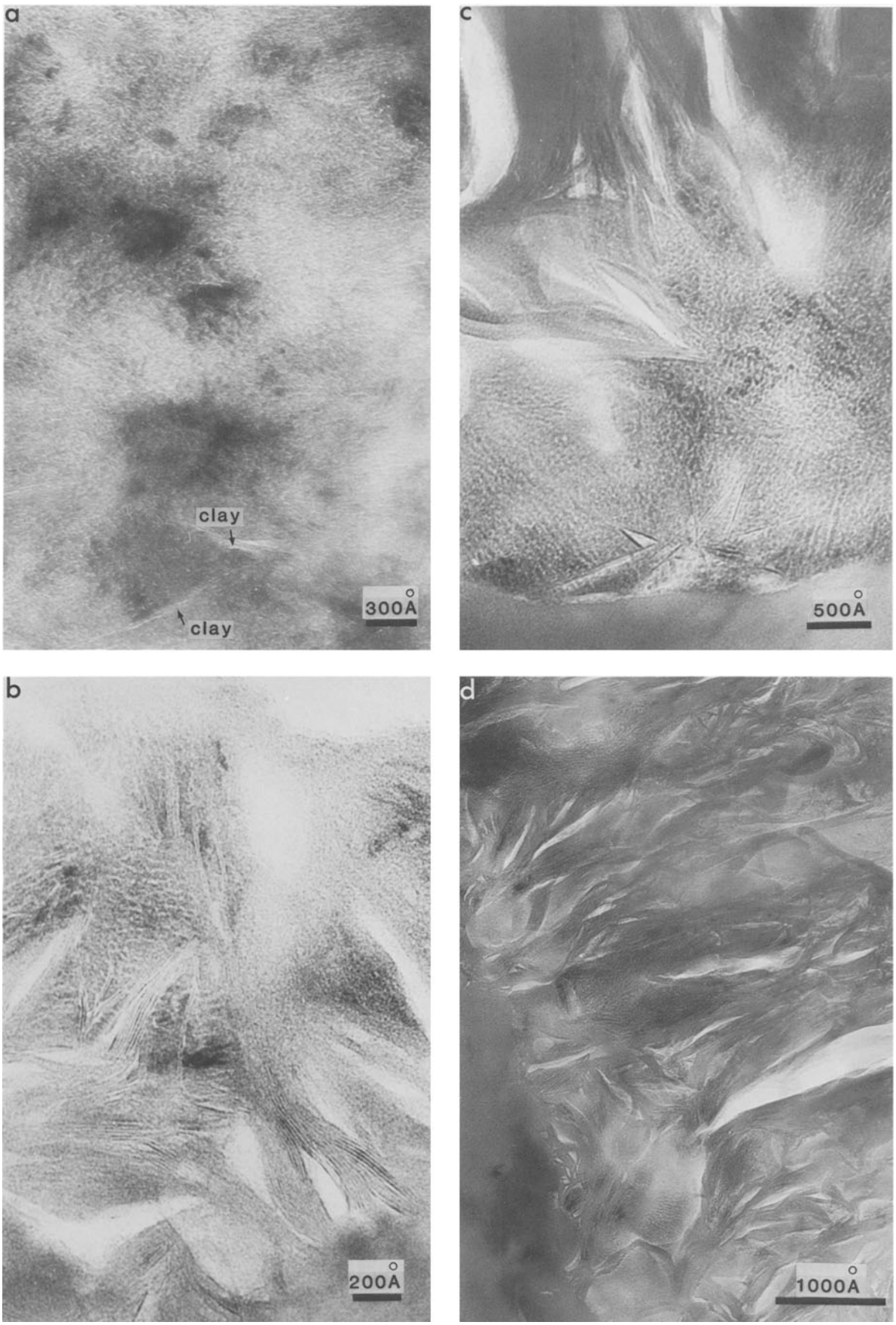


https://doi.org/10.1346/CCMN.1990.0380111 Published online by Cambridge University Press

tites from both profiles were Fe rich. The difference between smectites from the two profiles was the higher Fe content of the Bemboka smectite.

Electron microscopy and XRD indicated that halloysite and kaolinite also were abundant products of K-feldspar weathering. Spherical halloysite (distinguished from kaolinite by its morphology and from smectite by a 7–8-Å basal spacing and composition) commonly coexisted with smectite; tubular halloysite locally was found in cavities in more weathered samples. Kaolinite was the most abundant alteration product of the K-feldspar. Electron micrographs illustrated that this mineral formed irregular, commonly radiating laths in regions adjacent to those dominated by smectite and cell-textured material.

## DISCUSSION

Electron micrographs suggested that weathering of plagioclase and K-feldspar began at energetically favored sites, such as dislocations and twin planes. Dissolution was initially strongly controlled by the crystallography of the parent feldspar, resulting in the formation of sculpted surfaces honeycombed by prismatic pits and cracks. Similar processes have been well documented by many authors, particularly Berner and Holdren (1977, 1979).

In more highly weathered samples, the surfaces of large etch pits were much more irregular. Whereas defects were probably critical in providing initial pathways for solution and strain free-energy to promote reaction, the role of localized crystallographically controlled dissolution was greatly reduced as weathering proceeded. This reduction may have corresponded with a changeover to a surface-controlled reaction involving the cell-textured material, as alteration became more intense.

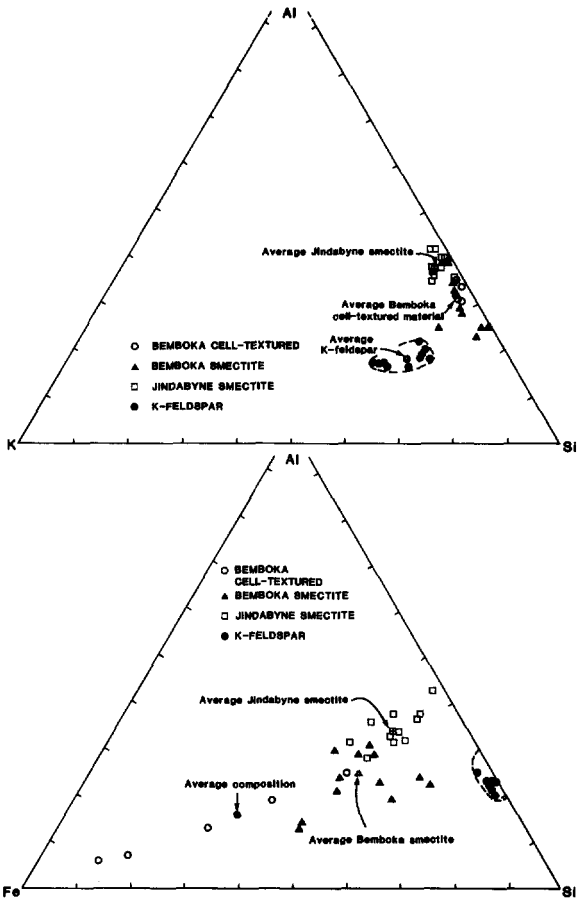


Figure 14. (upper) Triangular Al-K-Si composition diagram for K-feldspar, cell-textured material, and smectite. Average compositions illustrated in Figure 14 were semi-quantified and are included in the text. (lower) Triangular Al-Fe-Si composition diagram for K-feldspar and alteration products. Note pronounced Fe enrichment in cell-textured materials.

### *Protocrystalline material*

The initial alteration products of plagioclase, K-feldspar, and muscovite were transitory, apparently developed in response to the local physical and chemical conditions near the surfaces of the etch pits within the feldspar crystals. The cell-textured product of feldspar alteration had a variable composition and limited crystal order, as shown by the broad maxima in electron diffraction patterns and low contrast in TEM images. Although the electron diffraction lines were diffuse compared with those from feldspar, they were much sharper than those produced by the noncrystalline ion-beam-thinned edge of the sample. Furthermore, noncrystalline materials produced by electron irradiation differ both in appearance and diffraction characteristics from the cell-textured material described here. The cell-textured material resembled allophane in composition (Si:Al = 1.3–2.0; Henmi and Wada, 1976) and apparent lack of long-range order; however, the absence of pronounced spherical morphology, the presence of abundant iron, and the different diffraction pattern (allophane: d = 3.35, 2.25, 1.45 Å; Henmi and Wada, 1976) distinguished this material from allophane. The TEM data indicated that the cell-textured material was not noncrystalline, yet it lacked the long range order of a strictly crystalline material. The term 'protocrystalline' is used her to describe this material.

The intergrowth of abundant protocrystalline material with rare strips of clay only a few unit cells wide,

←

Figure 13. Transmission electron micrographs illustrating (a) cell-textured material adjacent to corroded K-feldspar; (b) narrow bands of clay formed within cell-textured material; (c) alignment within domains of cell-textured material; narrow strips and larger bands of clay; (d) progression from feldspar, to cell-textured material to larger elongate bands of clay.

the mixtures of clay and protocrystalline material, and the close spatial association of these areas with large crystals of smectite suggest that the protocrystalline material was a precursor of the clay. Although this protocrystalline material was not a volumetrically abundant weathering product of either feldspar, its presence at most feldspar margins suggests that it was an essential step in the conversion of the feldspar structure to smectite.

*Formation of smectite*

The replacement of both plagioclase and K-feldspar by smectite probably involved the formation of the protocrystalline intermediate, which may have contained polymers inherited from the feldspar structure. The retention of fragments containing more than three Al or Si cations is unlikely, because removal of K, Na, Ca probably destroyed the feldspar structure. Crystallization of the randomly oriented, initially narrow strips of smectite required change of most of the Al from 4-coordination in feldspar to 6-coordination, as well as a reorganization of tetrahedral and octahedral units and the addition of hydroxyl groups and water molecules.

The presence of a foliation within the protocrystalline material may reflect the initial stages of recrystallization (Figures 2 and 13), possibly representing the construction of the basic 2:1 layers. Tazaki and Fyfe (1987) described 'primitive' clays formed during feldspar weathering, which were somewhat similar to the smectites observed in the present study. The latter, however, were probably produced by recrystallization of protocrystalline material intermediate between the feldspar and the clay. Tazaki and Fyfe (1987) reported Fe compounds on, or adjacent to feldspar surfaces.

*Role of Fe*

The protocrystalline material that developed at the alteration front in both plagioclase and K-feldspar contained substantial (and variable) quantities of Fe. The very low Fe content of the parent minerals precludes the derivation of the Fe from the feldspar. Fe released by breakdown of other minerals, such as biotite, amphibole, or oxides, must either have been scavenged from solution by the protocrystalline material or adsorbed onto the feldspar surface and subsequently incorporated into its weathering products.

Although Fe was almost certainly not necessary for the weathering reactions to have proceeded, its presence probably had some effect, possibly similar to that reported for Al. The retarding effect of Al in solution on dissolution was reported by Chou and Wollast (1985). Casey *et al.* (1989) proposed that adsorption of a hydrated Al ion onto the feldspar surface results in the combination of two silanol groups and the elimination of a hydronium ion and water. The consequent repolymerization of the surface stabilizes the hydration layer. We suggest that adsorption of ferric iron may have promoted repolymerization in a manner similar to that suggested by Casey *et al.* (1989), resulting in the development of an Fe-enriched feldspar weathering product, such as the protocrystalline material.

Alternatively, if $Fe^{2+}$ had been present in solution, oxidation coupled with hydrolysis of water may have provided $H^+$ or $H_3O^+$, which attacked the feldspar structure, releasing K, Na, or Ca, as proposed by previous workers. The ferrolysis reaction may be written as:

$$2\,Fe(H_2O)_2{}^{2+}{}_{(aq)} + \tfrac{1}{2}\,O_2 \leftrightarrow 2\,FeO(OH)_{(s)} + 4\,H^+ + H_2O.$$

For Fe to participate in this manner, solutions in the weathering profile must have been, at least episodically, relatively reduced. The characteristics of a weathering solution (pH, oxygen content, dissolved ions) probably varied dramatically due to seasonal changes and in response to adjacent mineral weathering reactions, thereby explaining the mobilization of Fe and its precipitation in altered feldspar crystals.

In the ferric state, hydrolyzed iron may have also promoted feldspar weathering by buffering the pH. At pH 4–7, the most abundant $Fe^{3+}$ species is $[Fe(OH)_2 \cdot 4H_2O]^+$ (Lindsay, 1979). Polymerization of two such monomers releases a hydrogen ion according to the equation:

$$2[Fe(OH)_2 \cdot 4H_2O]^+ \leftrightarrow [Fe_2(OH)_5 \cdot 5H_2O]^+ + H^+ + 2H_2O.$$

The increase in pH resulting from $K^+$-$H_3O^+$ exchange would promote the ion monomers to coalesce into dimers (and higher molecular-weight polymers), releasing $H^+$ and restoring pH.

*Sequential development of feldspar weathering products*

The spatial distribution of plagioclase weathering products suggest a mineralogical pathway involving the replacement of feldspar by protocrystalline material, smectite, a second protocrystalline material, and spherical halloysite. After dissolution formed networks of cavities, Al and Si precititated from solution, resulting in the growth of tubular halloysite.

The breakdown of smectite may have been the result of increased throughflow of solution and a decrease in the pH of the local environment. The composition of the protocrystalline material that replaced it suggests that the smectite contained a range (at times very large) of Fe contents probably due to the accumulation of Fe that was released from smectite and not incorporated into halloysite.

Plagioclase should be replaced sequentially by smectite and kaolinite on the basis of phase diagrams, such as those of Feth *et al.* (1964), Loughnan (1969), Keller (1970), and those of Helgeson (1971) for higher-tem-

perature alteration (200°C). Similarly, the pathway for the replacement of muscovite by illite, smectite, and kaolinite can be traced on a $\log(aK^+/aH^+)$ vs. $\log a(SiO_2)$ diagram such as that of Garrels (1984). These pathways reflect the progressive change in composition of solutions within the rock during alteration, possibly reflecting increased porosity and throughflow of water as weathering proceeded. The overall trend appears to have been toward an assemblage of minerals in equilibrium with fluid having the composition and oxygen fugacity of meteoric water (Loughnan, 1969).

Most diagrams constructed for the alteration of K-feldspar predict the development of K-mica or illite as the intermediate phase between feldspar and kaolinite (e.g., Keller, 1970). In the profiles examined in the present study, K-feldspar did not develop secondary phases until late in weathering. The efficient removal of K at this stage may have promoted the replacement of K-feldspar by smectite rather than illite.

No evidence has been found to suggest that the abundant kaolinite formed by the weathering of K-feldspar crystallized from a protocrystalline material. Kaolinite developed in regions of sample adjacent to the smectite-protocrystalline intergrowths. In some regions in the altered feldspar, only kaolinite was present adjacent to the K-feldspar surface. Epitactic crystallization of kaolinite onto smectite may have taken place to some extent by the orientation and morphology of the kaolinite.

*Muscovite weathering*

The weathering of muscovite probably began after substantial alteration of the surrounding plagioclase had occurred. The experimental work Rausell-Colom *et al.* (1965) indicates that the removal of K from muscovite is extremely difficult and strongly dependent on the K content of the solution. Consequently, increased access of dilute water to the altering mica may have been required before K was substantially removed. Subsequently, individual layers of K-depleted muscovite were probably converted to smectite. The replacement of muscovite by smectite apparently occurred by direct exchange of components within the existing layers (Figure 9).

AEM analyses indicated that mica-derived illite and smectite contained small quantities of Mg, probably released from adjacent biotite by weathering reactions, and traces of Fe. This smectite differed from that derived from plagioclase by having a higher Al:Si, which may reflect the control exerted by the more aluminous composition of the parent. Smectite formed by the replacement of mica was, like the plagioclase-derived smectite, a transitory mineral, and was subsequently replaced by kaolinite.

Platy kaolinite developed from muscovite by crystallizing epitactically onto existing phyllosilicates, eventually forming kaolinite pseudomorphs (Figure 11). Transfer of material seems to have occurred via the solution, as no evidence was observed for a protocrystalline stage; however, the direct conversion of the structures cannot be completely ruled out. The distribution of kaolinite layers adjacent to pre-existing smectite and illite, rather than randomly throughout these minerals suggests that crystallization occurred by epitactic growth from solution. This mechanism of kaolinite crystallization has also been inferred for replacement of other 2:1 phyllosilicates in biotite-weathering reactions (Ahn and Peacor, 1987; Banfield and Eggleton, 1988).

*Crystallization of spherical and tubular halloysite and kaolinite*

Several models have been presented to explain the relationships between the various forms of halloysite, kaolinite, and noncrystalline material. Tazaki (1981) noted that noncrystalline material or allophane merged to form crinkled sheets containing >10% FeO. She proposed that sheets transformed to spherical particles by a reduction of $Fe^{3+}$. As tubular halloysite did not contain appreciable Fe, she suggested that tubes formed from an Fe-poor parent or by the removal of Fe from the crinkly film. Wilke *et al.* (1978) claimed that different degrees of enrollment result in the formation of platy, tubular, and spheroidal halloysite. Nagasawa and Miyazaki (1976) suggested that the morphology of halloysite is closely related to the parent rock type. Kurabayashi and others (in Sudo and Shimoda, 1978) described a sequence in which (rhyolitic) glass was transformed to allophane, then to 'chestnut-shell'-like particles that subsequently formed 10-Å tubular halloysite. Minato (1981) proposed that kaolinite formed from more acidic solutions than halloysite.

Within the sequences examined in this study, some evidence suggests that three separate mechanisms were responsible for the development of spherical halloysite, tubular halloysite, and kaolinite. Spherical halloysite probably crystallized from a protocrystalline precursor. Its growth pattern is consistent with that proposed by Eggleton (1987) for noncrystalline Al-Fe-Si oxyhydroxides. Tubular halloysite developed as a space-filling mineral, growing outward, probably via solution, from corroded feldspar surfaces, and kaolinite formed in the early stages of weathering appeared to have crystallized epitactically onto existing phyllosilicates. No chemical distinction between spherical and tubular halloysite was detected using the STEM with a spot size comparable with that of a single spherical halloysite particle. Crystallization in the presence of abundant water, such as in cavities in feldspar, and within the presumably hydrous protocrystalline material, apparently favored the growth of halloysite. Lower activity of water, such as within micas and as encountered during the dry stages in periodic wetting and drying in the profile, should have promoted the crystallization

of kaolinite. These factors may explain the development and distribution of the different forms of halloysite and kaolinite within altering feldspars. The extent to which this mechanism provides a general explanation for the coexistence of these minerals is not known.

## SUMMARY AND CONCLUSIONS

Several series of transitional phases formed during the weathering of K-feldspar, plagioclase, and included muscovite in granodiorite. In some of these sequences the direct transformation of structures was inferred, some involved the formation of protocrystalline material, and others appear to have proceeded by dissolution and reprecipitation. Transitional minerals crystallized in local environments within the feldspar crystals. Because a chemical distinction could be made between the smectite produced by weathering of the different minerals although they existed in close proximity, the distinct microenvironments probably formed on a sub-micrometer scale. The changing stability (or metastability) of weathering products was probably due to the increased access of dilute oxygenated solutions as etch pits became enlarged and formed networks. Consequently, intermediate products of weathering provided only temporary sites for elements, such as Ca, K, (Na), Mg, Fe, and Si, which were subsequently removed in solution or precipitated as other alteration products.

A protocrystalline phase formed adjacent to many of the corroded feldspar surfaces. In some regions this cell-textured material coexisted with very narrow bands of clay, which probably was the initial nucleation product in the recrystallization sequence that produced larger, curved bunches of smectite.

The assemblage of clay minerals produced by weathering of feldspars and muscovite included spherical halloysite, tubular halloysite, and platy kaolinite. The distribution of these three chemically indistinguishable (by AEM) minerals suggests that their morphologies were the direct result of the manner in which they crystallized; tubes formed in cavities by growth from solution, spherical particles developed from protocrystalline precursors, and kaolinite formed largely by templating onto existing phyllosilicate structures.

## ACKNOWLEDGMENTS

We thank B. Hyde of the Research School of Chemistry for access to the transmission electron microscope and P. Barlow, J. Preston, and N. Ware for technical assistance. Helpful suggestions were provided by D. Varkevisser, R. F. Martin, R. J. Gilkes, G. D. Guthrie, and E. S. Ilton and an anonymous reviewer. F. A. Mumpton is thanked for editorial handling. D. Goodchild of the C.S.I.R.O. Division of Plant Industry made available the STEM and assisted with its operation.

## REFERENCES

Aagaard, P. and Helgeson, H. C. (1982) Thermodynamic and kinetic constraints on reaction rates among minerals and aqueous solutions: I. Theoretical considerations: *Amer. J. Sci.* **282,** 237–285.

Ahn, J. H. and Peacor, D. R. (1987) Kaolinitization of biotite: TEM data and implications for an alteration mechanism: *Amer. Mineral.* **72,** 353–356.

Anand, R. R., Gilkes, R. J., Armitage, T., and Hillyer, J. (1985) The influence of microenvironment on feldspar weathering in lateritic saprolite: *Clays & Clay Minerals* **33,** 31–46.

Banfield, J. F. (1985) The mineralogy and chemistry of granite weathering: M.Sc. thesis, Australian National University, Canberra, Australia, 229 pp.

Banfield, J. F. and Eggleton, R. A. (1988) A transmission electron microscope study of biotite weathering: *Clays & Clay Minerals* **36,** 47–60.

Banfield, J. F. and Eggleton, R. A. (1989) Apatite replacement and rare earth mobilization, fractionation, and fixation during weathering: *Clays & Clay Minerals* **37,** 113–127.

Beams, S. D. (1980) Magmatic evolution of the southeast Lachlan Fold Belt, Australia: Ph.D. thesis, Australian National University, Canberra, Australia, 257 pp.

Berner, R. A. and Holdren, G. R., Jr. (1977) Mechanism of feldspar weathering: I. Some observational evidence: *Geology* **5,** 369–372.

Berner, R. A. and Holdren, G. R., Jr. (1979) Mechanism of feldspar weathering: II. Observations of feldspars from soils: *Geochim. Cosmochim. Acta* **43,** 1173–1186.

Carroll, D. (1970) *Rock Weathering:* Plenum Press, New York, 203 pp.

Casey, W. H., Westrich, H. R., and Arnold, G. W. (1989) Surface chemistry of labradorite feldspar reacted with aqueous solutions at pH = 2, 3, and 12: *Geochim. Cosmochim. Acta* **52,** 2795–2807 (in press).

Chou, L. and Wollast, R. (1985) Steady-state kinetics and dissolution mechanisms of albite: *Amer. J. Sci.* **285,** 963–993.

Churchman, G. T. (1980) Clay minerals formed from micas and chlorite in some New Zealand soils: *Clay Miner.* **15,** 59–76.

Churchman, G. T., Whitton, J. S., Claridge, G. G. C., and Theng, B. K. G. (1984) Intercalation method using formamide for differentiating halloysite from kaolinite: *Clays & Clay Minerals* **32,** 241–248.

Cliff, G. and Lorimer, G. W. (1975) The quantitative analysis of thin specimens: *J. Microscopy* **103,** 203–207.

Correns, C. W. and Von Englehardt, W. (1938) Neue Untersuchungen über die Verwitterung des Kalifeldspates: *Chemie der Erde* **12,** 1–22.

Eggleton, R. A. (1987) Noncrystalline Fe-Si-Al-oxyhydroxides: *Clays & Clay Minerals* **35,** 29–37.

Eggleton, R. A. and Buseck, P. R. (1980) High-resolution electron microscopy of feldspar weathering: *Clays & Clay Minerals* **28,** 173–178.

Eswaran, H. and Bin, W. C. (1978) A study of a deep weathering profile on granite in peninsular Malaysia: III. Alteration of feldspars: *Soil Sci. Soc. Amer. J.* **42,** 154–158.

Feth, J. H., Roberson, C. E., and Polzer, W. L. (1964) Sources of mineral constituents in water from granitic rocks, Sierra Nevada, California, and Nevada: *U.S. Geol. Surv. Water Supply Pap.* **1531-1,** 170 pp.

Fieldes, M. and Swindale, L. D. (1954) Chemical weathering of silicates in soil formation: *J. Sci. Tech. New Zealand* **56,** 140–154.

Frederickson, A. F. (1951) Mechanism of weathering: *Geol. Soc. Amer. Bull.* **62,** 221–232.

Garrels, R. M. (1984) Montmorillonite/illite stability diagrams: *Clays & Clay Minerals* **32,** 161–166.

Garrels, R. M. and Howard, P. (1959) Reactions of feldspar and mica with water at low temperature and pressure: in *Clays and Clay Minerals, Proc. 6th Natl. Conf., Berkeley, California, 1957,* A. Swineford, ed., Pergamon Press, New York, 66–88.

Guilbert, J. M. and Sloane, R. L. (1968) Electron optical study of hydrothermal fringe alteration of plagioclase in quartz monzonite, Butte District, Montana: *Clays & Clay Minerals* **16,** 215–221.

Guthrie, G. D. and Veblen, D. R. (1989) High resolution transmission electron microscopy of mixed-layer illite/smectite: Computer simulations: *Clays & Clay Minerals* **36,** 1–11.

Helgeson, H. C. (1971) Kinetics of mass transfer among silicates and aqueous solutions: *Geochim. Cosmochim. Acta* **35,** 421–469.

Helgeson, H. C., Murphy, W. M., and Aagaard, P. (1984) Thermodynamic and kinetic constraints on reaction rates among minerals and aqueous solutions. II. Rate constants, effective surface area, and the hydrolysis of feldspar: *Geochim. Cosmochim. Acta* **48,** 2405–2432.

Henmi, T. and Wada, K. (1976) Morphology and composition of allophane: *Amer. Mineral.* **61,** 379–390.

Holdren, G. R., Jr. and Berner, R. A. (1979) Mechanism of feldspar weathering. I. Experimental studies: *Geochim. Cosmochim. Acta* **43,** 1161–1171.

Keller, W. D. (1970) Environmental aspects of clay minerals: *J. Sed. Petrol.* **40,** 788–813.

Keller, W. D. (1978) Kaolinization of feldspar as displayed in scanning electron micrographs: *Geology* **6,** 184–188.

Lagache, M., Wyart, J., and Sabatier, G. (1961) Dissolution des feldspaths alcalins dans l'eau pure ou chargée de $CO_2$ à 200°C: *C. R. Acad. Sci. Paris* **253,** 2019–2022.

Lin, F.-C. and Clemency, C. V. (1981) The kinetics of dissolution of muscovites at 25°C and 1 atm, $CO_2$ partial pressure: *Geochim. Cosmochim. Acta* **45,** 571–576.

Lindsay, L. (1979) *Chemical Equilibrium in Soils:* Wiley, New York, 449 pp.

Lodding, W. (1972) Conditions for the direct formation of gibbsite from K-feldspar. Discussion: *Amer. Mineral.* **57,** 292–294.

Loughnan, F. C. (1969) *Chemical Weathering of Silicate Minerals:* Elsevier, Amsterdam, 273 pp.

Lundstrom, I. (1970) Etch pattern and twinning in two plagioclases: *Arkiv Mineralogi och Geologi* **5,** 63–91.

Marshall, C. E. (1962) III. Reactions of feldspars and micas with aqueous solutions: *Econ. Geol.* **57,** 1219–1227.

Minato, H. (1981) On the problem of genesis in kaolinite and halloysite by hydrothermal water: *J. Min. Soc. Japan* **13,** (in Japanese) Abstracted in *Mineral. Abst.* **32,** 81-0150, 1981.

Nagasawa, K. and Miyazaki, S. (1976) Mineralogical properties of halloysite as related to its genesis: in *Prog. Abst., Int. Clay Conf., Mexico City, 1976,* Univ. Nac. Auton. Mexico., 223–224.

Nixon, R. A. (1979) Differences in incongruent weathering of plagioclase and microline—Cation leaching versus precipitates: *Geology* **7,** 221–224.

Parham, W. E. (1969) Formation of halloysite from feldspar: Low temperature artificial weathering versus natural weathering: *Clays & Clay Minerals* **17,** 13–22.

Petrovic, R. (1976a) Rate control in feldspar dissolution. I. Study of residual feldspar grains by X-ray photoelectron spectroscopy: *Geochim. Cosmochim. Acta* **40,** 537–548.

Petrovic, R. (1976b) Rate control in feldspar dissolution. II. The protective effect of precipitates: *Geochim. Cosmochim. Acta* **40,** 1509–1521.

Petrovic, R., Berner, R. A., and Goldhaber, M. B. (1976) Rate control in dissolution of alkali feldspars. I. Study of residual grains by X-ray photoelectron spectroscopy: *Geochim. Cosmochim. Acta* **40,** 537–548.

Proust, D. and Velde, B. (1978) Beidellite crystallization from plagioclase and amphibole precursors. Local and long-range equilibrium during weathering: *Clay Miner.* **13,** 199–209.

Rausell-Colom, J., Sweatman, T. R., Wells, C. B., and Norrish, K. (1965) Studies in the artificial weathering of mica: in *Proc. 11th School Agr. Sci., Nottingham, 1965,* Butterworth, London, 40–72.

Rimsaite, J. (1979) Natural amorphous materials, their origin and identification procedures: in *Proc. Int. Clay Conf., Oxford, 1978,* M. M. Mortland and V. C. Farmer, eds., Elsevier, Amsterdam, 567–577.

Siefert, K. E. (1967) Electron microscopy of etched plagioclase feldspars: *Amer. Ceramics Soc. J.* **50,** 660–661.

Sudo, T. and Shimoda, S. (1978) *Clays and Clay Minerals of Japan:* Kodansha Ltd., Tokyo, 326 pp.

Tardy, Y., Bocquier, G., Parquet, H., and Millot, G. (1973) Formation of clay from granite and its distribution in relation to climate and topography: *Geoderma* **10,** 271–284.

Tazaki, K. (1981) Analytical electron microscope studies of halloysite formation processes—Morphology and composition of halloysite: in *Proc. Int. Clay Conf., Bologna, Pavia, 1981,* H. van Olphen and F. Veniale, eds., Elsevier, Amsterdam, 573–584.

Tazaki, K. and Fyfe, W. S. (1987) Primitive clay precursors formed on feldspar: *Canadian J. Earth Sci.* **24,** 506–527.

Tsuzuki, Y. and Kawabe, I. (1983) Polymorphic transformations of kaolin minerals in aqueous solutions: *Geochim. Cosmochim. Acta* **47,** 59–66.

t'Serstevens, A., Rouxhet, P. G., and Herbillon, A. J. (1964) Alteration of mica surfaces by water and solutions: in *Clays and Clay Minerals, Proc. 13th Natl. Conf., Madison, Wisconsin, 1964,* W. F. Bradley and S. W. Bailey, eds., Pergamon Press, New York, 401–411.

White, A. J. R., Williams, I. S., and Chappell, B. W. (1977) Geology of the Berridale 1:100,000 Sheet 8625: Geol. Surv. New South Wales, Dept. of Mines Publ.

Wilke, B. S., Schwertmann, U., and Murad, E. (1978) An occurrence of polymorphic halloysite in granite saprolite of the Bayerischer Wald, Germany: *Clay Miner.* **13,** 67–77.

Wilson, M. J., Bain, D. C., and McHardy, W. J. (1971) Clay mineral formation in deeply weathered boulder conglomerate in northeast Scotland: *Clays & Clay Minerals* **19,** 345–352.

Wollast, R. (1967) Kinetics of the alteration of K-feldspar in buffered solutions: *Geochim. Cosmochim. Acta* **31,** 635–648.

Wollast, R. and Chou, L. (1985) Kinetic study of the dissolution of albite with a continuous flow-through fluidized bed reactor: in *The Chemistry of Weathering,* J. I. Drever, ed., Reidel, Dordrecht, The Netherlands, 75–96.

*(Received 29 February 1988; accepted 19 May 1989; Ms. 1767)*